Analysis of the Effect of Changes in Pitch Ratio and Number of Blades on Cavitation on CPP

Mohammad Danil Arifin[1], Danny Faturachman [2], Fanny Octaviani [3], Karina A Sulaeman[4]

Abstract*— Cavitation is a detrimental phenomenon to ship operations because it causes many losses. It caused some effects i.e decreased propeller efficiency, damaged propeller material, lower ship speed, vibration, and extreme noises. In that regard, this research conducts cavitation analysis on controllable pitch propeller (CPP) by varying number of blade i.e. 3, 4 and 5 blades; diameter i.e. 30, 40 cm and 50 cm; also pitch i.e 0.4, 0.6 and 0.8. The research method is carried out by the author in this study by conducting a simulation method based on the CFD approach. The simulation process consists of 3 stage-post processor, solver manager, and post-processor. From the simulation based on the CFD approach result, it was found that propeller rotation has an effect on the pressure ratio value. As the propeller rotation increase, the value of the pressure ratio will increase as well. The value of the pressure ratio in propeller design affects the cavitation area that occurs in the propeller. The percentage of the cavitation area on the propeller has an increasing tendency with the number of blades, rotation, and pitch. On the propeller with diameter 300 mm, 3 blades, pitch 0.8 at rotation 125 rpm no indication of cavitation, then it increases to 1.41% at rotation 175 rpm and keeps getting higher at rotation 225 to be 4.22% from total propeller expanding area. Whereas at rotation 225 rpm and pitch 0.4 is 3.38 %, then it becomes 3.85 % at pitch 0.6, which is getting bigger at pitch 0.8 that is 4.22 %.

Keywords— Ambient Temperature, Cavitation, CFD Approach, Controllable Pitch Propeller (CPP), Propeller Design, Simulation

I. INTRODUCTION

During recent year's great advancement of computer performance, Computational Fluid Dynamics (CFD) methods for solving the Reynolds Averaged Navier-Stokes (RANS) equation have been increasingly applied to various marine propeller geometries, and more and more research articles have been published [1].

While these studies have shown great advancement in technology, some issues still need to be addressed for more practicable procedures. These include mesh generation strategies and turbulence model selection. With the availability of superior hardware, it becomes possible to model complex fluid flow problems like propeller flow and cavitation [2].

For many years, propellers were predicted using the lifting line theory, where the blade was represented by a vortex line and the wake by a system of helicoidal vortices. With the advent of computers, numerical methods developed rapidly from the 1960s onwards. The first numerical methods were based on the lifting line theory, and later the lifting surface model was developed. Salvatore et al. [3] presented the theoretical basis of the lifting-line theory based on perturbation methods.

Fujiyama [4] has analyzed the unsteady cavitating flow of HSP-II and CP-II propeller at behind-hull condition both in the model and full scale, using commercial software SC/Tetra v13. The results show that the unsteady propeller cavitation phenomena can be captured in the numerical calculation.

Kawakita et al. [5] has developed energy-saving devices that improve the propulsive performance and fuel consumption of ships, including reaction fins for low-speed full ships and stator fins for high-speed slender ships by developed computational fluid dynamics (CFD) technologies that analyze and evaluate the cavitation occurrence characteristics of propellers equipped with energy-saving devices as a unit, including the hull and rudder.

Long [6] has researched the propeller cavitating flow behind the hull, analyzed the vorticity distribution and particle tracks as well, using commercial software CFX and Zwart cavitation model. The cavitation patterns predicted resemble well with the experimental observations, with some over-prediction of the cavitation area. Pereira et al. [7] presented an experimental and theoretical investigation on a cavitating propeller in uniform inflow. Flow field investigations by advanced imaging techniques are used to extract quantitative information on the cavity extension. Pereira and Sequeira [8] developed a turbulent vorticity-confinement strategy for RANSbased industrial propeller-flow simulations. The methodology aims at an improved prediction of tip vortices, which are the origin of cavitation.

Arifin et al. [9] [10] analyzed the cavitation on the propeller by using the simulation based on the CFD approach in order to get the best configuration for the effectiveness of the propeller. The numerical or experimental analysis and comparison of results highlight the peculiarities of propellers, the possibility to increase efficiency and reduce cavitation risk, in order to exploit the design approaches already well-proven for conventional propellers also in the case of unconventional geometries. The simulated flow pattern agrees with the experimental data in most cases. However, there is limited research focused on controllable pitch propeller (CPP).

Mohammad Danil Arifin, Department of Marine Engineering, Darma Persada University, Jakarta, 13450, Indonesia.
E-mail: danilarifin.mohammad@gmail.com
Danny Faturachman, Department of Marine Engineering, Darma Persada University, Jakarta, 13450, Indonesia.
E-mail: fdanny30@yahoo.com
Fanny Octaviani, Department of Naval Architecture, Darma Persada University, Jakarta, 13450, Indonesia.
E-mail:fanny_octaviani@yahoo.com
Karina A Sulaeman, Department of English Language and Culture, Darma Persada University, Jakarta, 13450, Indonesia.
E-mail:karina_adinda@yahoo.co.id

Controllable Pitch Propeller (CPP) is one of the developments of the propeller. CPP is a type of propeller that can change the pitch or angle of its blade. This angle of the blade will be adjusted to the need of the ship [11] [12]. CPP has several advantages compared to other types of propellers. The use of CPP (by modifying the pitch) will help us change the engine rotation easily to reduce vibration and noise in the engine, just like the pitch that can be modified to reduce cavitation in various engine rotations [13] [14].

So in this present paper, the simulation method based on the CFD approach is conducted to analyze the cavitation on the CPP against changes in working pitch and number of blades, and compare the cavitation on changes in working pitch and amount angles on the CPP through the simulation results. By varying number of blade i.e. 3, 4 and 5 blades; diameter i.e. 30, 40 cm and 50 cm; also pitch i.e 0.4, 0.6 and 0.8, the simulation results are compared.

II. METHOD

In this research, the simulation method by using a CFD approach is used by varying number of blade i.e. 3, 4 and 5 blades; diameter i.e. 30, 40 cm and 50 cm; also pitch i.e 0.4, 0.6 and 0.8. Geometric modeling of propeller is carried out using PropCad software. This study was conducted by considering the following aspects:

A. Basic Equation of Computational Fluid Dynamic

Implementation on used software is Computational Fluid Dynamic (CFD) covering inputs of fluid condition as flowing media, i.e:

1) Boundary Condition Inlet
   Is path fluid flowing input in normal condition without any phenomenon occurred.
   a) Mass and Momentum
      The momentum that occurs in fluid flow is influenced by mass and velocity with velocity vectors U, V, and W.
      The direction engaged in treating the boundary is the normal direction to the domain. Component of flow velocity (Cartesian Velocity Vector) is by resultant:

$$U_{inlet} = U_{spec}{}^{j} + V_{spec}{}^{i} + W_{spec}{}^{k} \quad (1)$$

   b) Total Pressure
      Total pressure, plot for fluid is defined as:

$$P_{tot} = P_{static} \quad (2)$$

   c) Speed of Mass Flow Rate
      The mass flow rate limit, determined through the direction of the component where the influx is mass, is calculated using the formula:

$$\rho U = m / \int_s Da \quad (3)$$

2) Boundary of Outlet Condition
   a) Outlet Speed
      The outlet boundary velocity component is a cartesian velocity vector component

$$U_{outlet} = U_{spec}{}^{i} + V_{spec}{}^{j} + W_{spec}{}^{k} \quad (4)$$

   b) Outlet of Fluid Pressure
      The outlet fluid pressure is static inlet pressure plus the occurred changing pressure

$$P_{tot} = P_{static} + \frac{1}{2}\rho U^2 \quad (5)$$

3) Boundary of Wall Condition
   a) Walk Relative Static Pressure is:

$$Pav = PdA\ A \int PdA \quad (6)$$

   b) Mass Flow Rate Out
      The mass distribution in the wall area is determined by the mass flow:

$$m = p\ A \quad (7)$$

      where the value of F is calculated so that M tot = $\sum_{all}$ m, and the force is a total mass flow in the boundary wall. Therefore F can be used as follows :

$$F = PdA \quad (8)$$

B. Cavitation

Cavitation is defined as the forming process of the vapor phase of a liquid when the liquid is getting reduced pressure at a fixed ambient temperature. Generally, the liquid is considered to get cavitation if there is a bubble inside the liquid formed due to reduced pressure [9] [10] [15]. There are many causes that can lead to cavitation. The most common example is boiling water. In boiling water, the vapor pressure increases due to increasing water temperature.

In marine hydrodynamic cavitation generally caused by fluid flow. That flowing is two-phase flowing consisting of liquid and its liquid steam. Phase transition is created due to changes in hydrodynamic pressure.

Figure 1 shows the cavitation mechanism when a foil is put at a small hitting angle in the steady two-dimensional flow without viscosity. Far ahead from this cross-section.

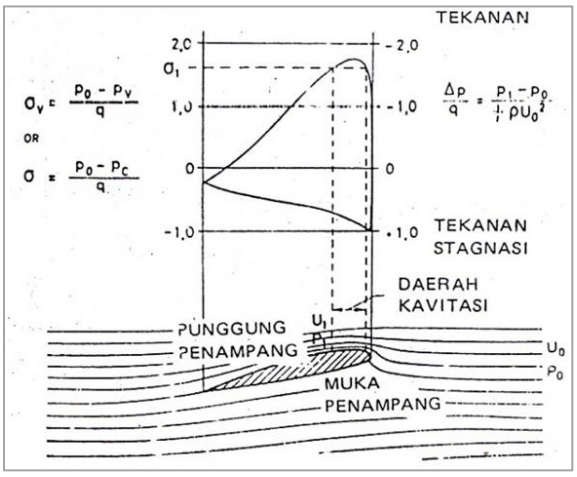

Figure. 1. Flow and pressure around the airfoil

The velocity is steady and uniform are considered U_0 and total pressure p_0. For a particular flow line, the Bernoulli theory provides:

$$\rho_0 + {}^1\!/_2\,\rho U_0 = constant \quad (9)$$

Therefore, at any point of the flow line, the following equations apply p_1 and U_1 is pressure and velocity at that point:

$$\rho_0 + {}^1\!/_2\,\rho U_1^2 = \rho_0 + {}^1\!/_2\,\rho U_0^2 \quad (10)$$

The change in pressure at that point is

$$\Delta p = p_1 - p_0 = {}^1\!/_2\,\rho(U_0^2 - U_1^2) \quad (11)$$

If U_1 is faster than U_0 so p_1 will be smaller than p_0 so Δp will get the more negative points. At point S in front of the nose, the flow will be split. The fluid that follows the flow line will rotate at 90◦ and loses the entire speed of its momentum in the direction according to its movement along the flow line. Thus, at that S point (stagnation point) the velocity U_1 is zero. q is the stagnant flow. The pressure at the point on the backside of foil is:

$$\Delta p = p_1 - p_0 = {}^1\!/_2\,\rho U_0^2 = q \quad (12)$$

and q is stagnation of that flow pressure on the back of the blade is

$$p_1 = p_0 + {}^1\!/_2\,\rho(U_0^2 - U_1^2) = p_0 + \Delta p \quad (13)$$

So, p_1 will be zero if,

$$-p_0 = \Delta p \quad (14)$$

This means that flow will break at that point considering that water cannot withstand tension. Bubbles and cavity in cavitation will appear if,

$$p_v = p_0 + \Delta p \quad (15)$$

Pv is the water vapor pressure when water starts to boil. Because of that cavitation will occur if

$$-\Delta p > p_0 - p_v \quad (16)$$

and

$$\frac{\Delta p}{q} > \frac{p_0 - p_v}{q} = \sigma_v \quad (17)$$

Δp is the pressure change and the geometry characteristic of flowing σv is called vapor cavitation rate. In this figure number p_0 is static pressure which is the sum of the pressure hydrostatic and atmosphere. *Pv* vapor pressure is not affected by temperature. stagnation pressure q depends on the mass of fluid type and velocity.

C. CFD Approach Simulation

1) Initial Stage

This initial stage determines formula and problem identification to deal with. Furthermore, it will be a reference to formulate the implemented method. The discussed problem is how to analyze cavitation on changing of pitch system and number of blades in controllable pitch propeller (CPP)

2) Model Variation

Making of model propeller uses PropCad software. Propeller design is conducted by varying numbers of blades, diameter, and pitch propeller. The number of blades in this propeller design is 3, 4, and 5 blades by varying diameters of 30, 40, and 50 cm also by the varying pitch of propeller that is 0.4, 0.6, and 0.8. Below is the result of geometry design visualization in ANSYS software as shown in Figure 2. The number of blades from propeller design is 3, 4, and 5 with varying diameter is 30, 40, and 50 cm, also by varying propeller pitch around 0.4, 0.6, dan 0.8.

The angle of attack of the propeller is calculated by using the following equation:

$$\theta = \tan^{-1}\frac{P/D_{0.7}}{2\pi R_{0.7}/D} = \tan^{-1}\frac{P/D_{0.7}}{0.7\pi} \quad (18)$$

So, the angle of attack of the varying model is shown as follows:

TABLE 1.
VARIATION OF ANGLE OF ATTACK

D	$P/D_{0.7}$	$(P/D_{0.7})/(0.7R)$	θ(rad)	θ(degree)
30	0.4	0.18189	0.1799	10.3
	0.6	0.27284	0.2664	15.3
	0.8	0.36378	0.3489	20.0
40	0.4	0.18189	0.1799	10.3
	0.6	0.27284	0.2664	15.3
	0.8	0.36378	0.3489	20.0
50	0.4	0.18189	0.1799	10.3
	0.6	0.27284	0.2664	15.3
	0.8	0.36378	0.3489	20.0

3) Simulation using CFD

The model of the ship and propeller developed in the previous chapter is simulated by using CFD software. Data gathered from the simulation process will be used as validation by using other software. There are several steps to conduct the simulation process based on the CFD approach.

a) Pre-Processor

Pre-Processor is step is early-stage where programming language of model design will be translated by Solver Manager. The model will be formed in such a way that several parts can limit conducted fluid flow and make the model as an object flowed by fluid.

In this case, there are 2 parts in modeling as an object and to make a boundary for fluid. From the two parts object and the boundary as shown in Figure 3(a), then make fluid flow direction, they are inlet dan outlet flow so that fluid flow will touch the object.

The object is a wall CFX language. The developed model then will be imported into CFX software, whereas the previous model is the only surface but after imported into CFX it becomes solid.

The next step is meshing. In CFX, the developed model will be conditioned based on the real situation. For analysis purposes, it needs to enter the domain or conditioned model as shown in Figure 3(b).

Examples of domains are type, temperature, velocity, and a number of iterations.

b) Solver Manager

Solver manager is the second step to CFX. This step is to function as a file translator from .def format to be res format. The next step can be translated by post-processor [8][9].

c) Post-Processor

At post-processor step will show the calculation result conducted in the Solver Manager phase. The result is numerical data visualizing fluid flow on the model. Numerical data taken is the characters of fluid and its variables.

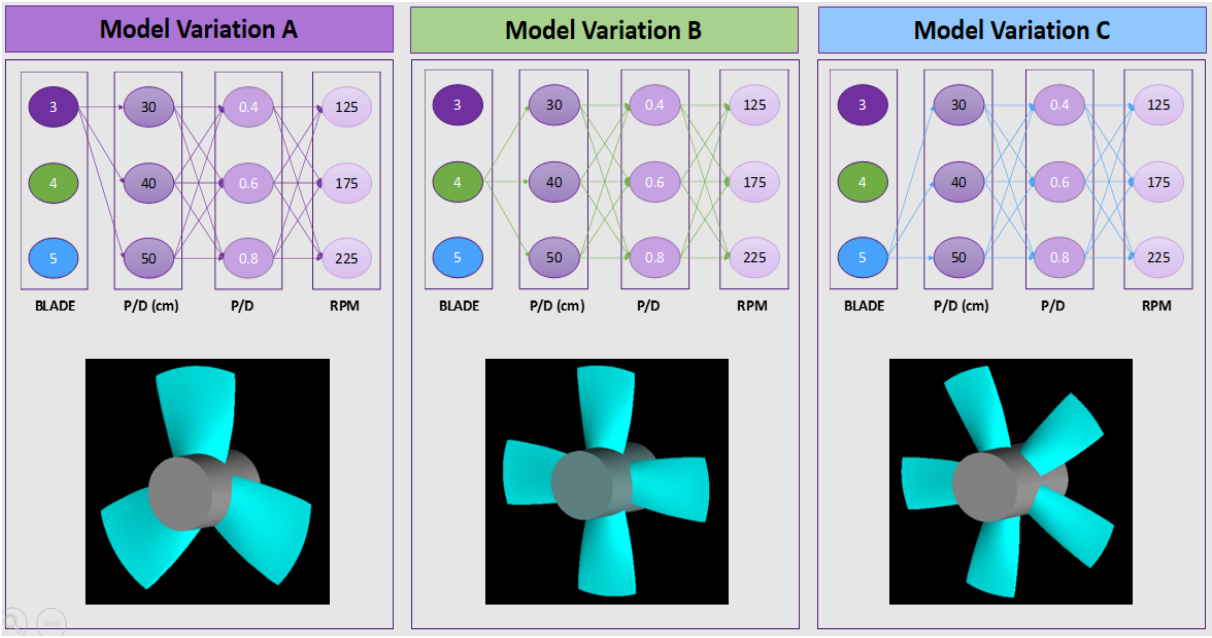

Figure. 2. Propeller geometry with 3, 4 ,5 blades

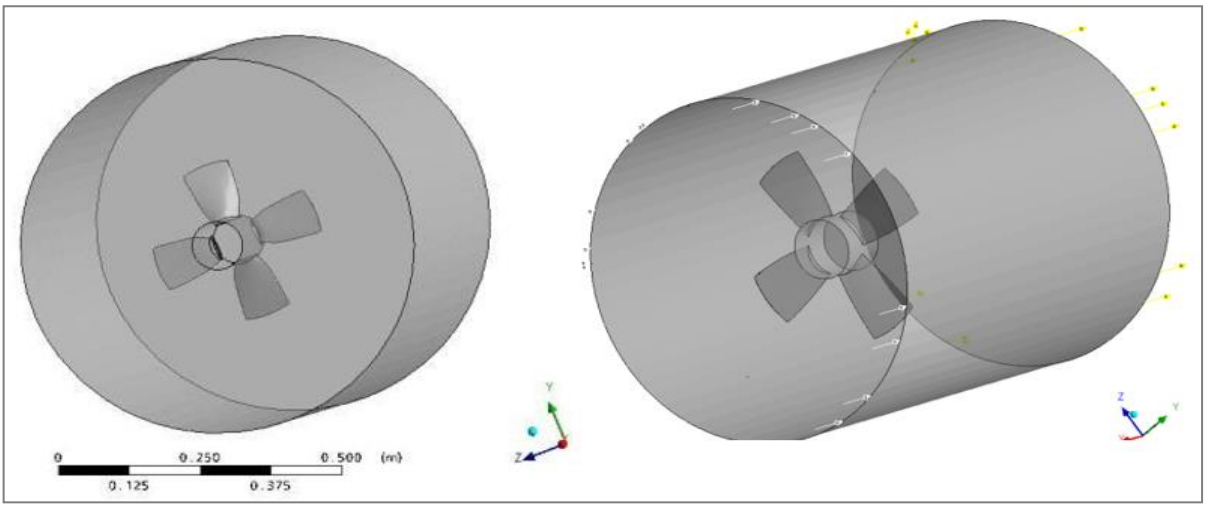

Figure. 3. (a) Object and boundary (left), (b) Propeller model domain (right)

III. Results and Discussion

3.1 Propeller Pressure

1) Propeller Pressure Analysis

CFD simulation is conducted on the propeller to identify the ratio of the pressure value on the face and back propeller after completing several variations i.e. diameter, pitch, propeller rotation, whereas CFD can display pressure profile. CFD simulation will show characteristics inclination of cap fins of each design of given rotation variation. The example of the CFD simulation results for propeller design variations on pressure analysis is shown in the following Figure.

Figure 4 to 6 shows the pressure contour visualization on post-processor face and back part of rotation 225 rpm with 3 blades, d = 400 mm, and of pitch i.e. 0.4, 0.6, 0.8. However, Figure 7 to 9 shows the pressure contour visualization on post-processor face and back part of rotation 225 rpm with 4 blades, d = 400 mm, and variation of pitch i.e. 0.4, 0.6, 0.8. Furthermore, Figure 10 to 12 shows the pressure contour visualization on post-processor face and back part of rotation 225 rpm with 5 blades, d = 400 mm, and variation of pitch i.e. 0.4, 0.6, 0.8. The calculation results of the pressure ratio by varying propeller geometry shows in the following tables on the next section.

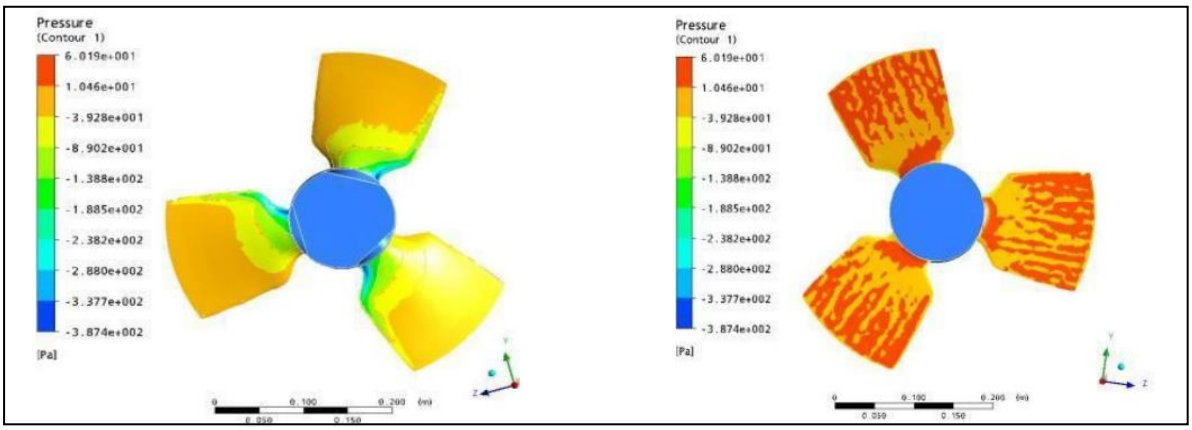

Figure. 4. Pressure Contour at face and back propeller with 3 blades, 225 rpm, d=400 mm, pitch = 0.4

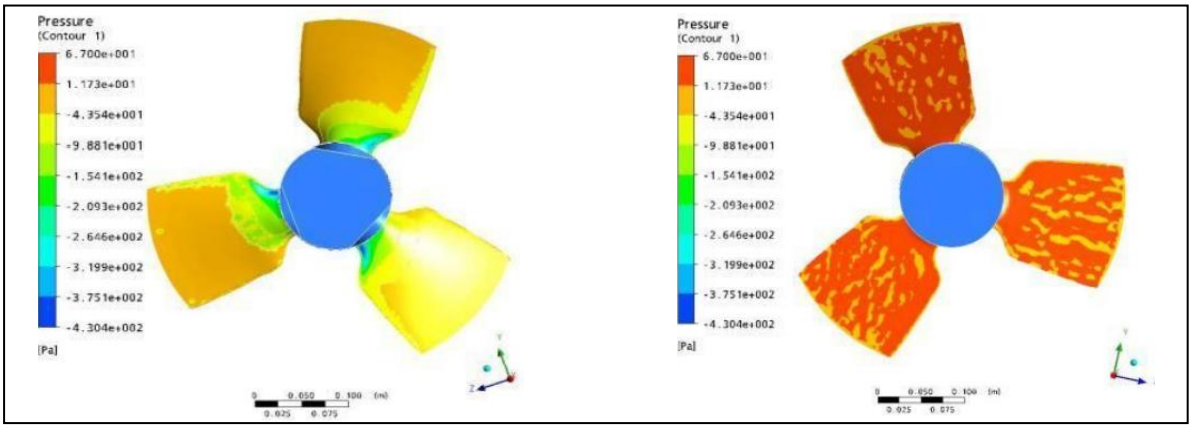

Figure. 5. Pressure Contour at face and back propeller with 3 blades, 225 rpm, d=400 mm, pitch = 0.6

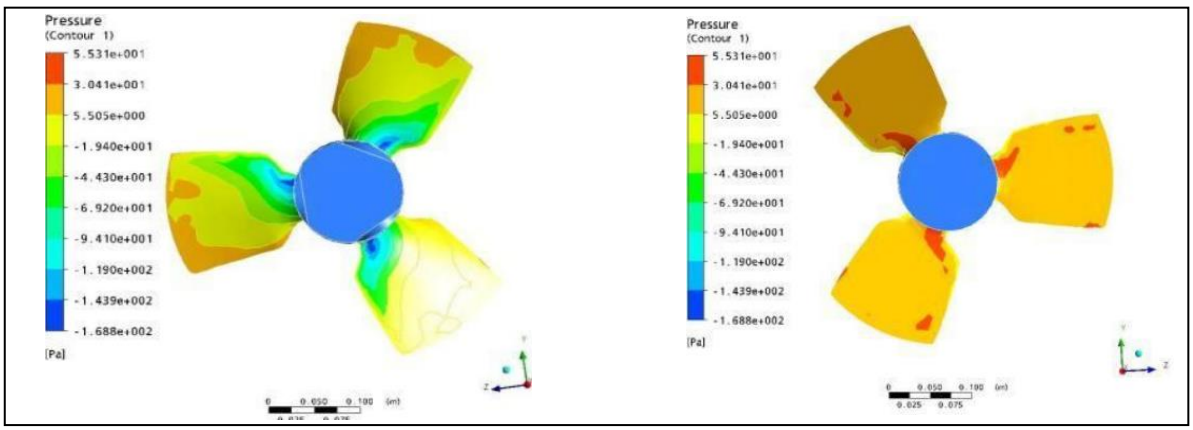

Figure. 6. Pressure Contour at face and back propeller with 3 blades, 225 rpm, d=400 mm, pitch = 0.8

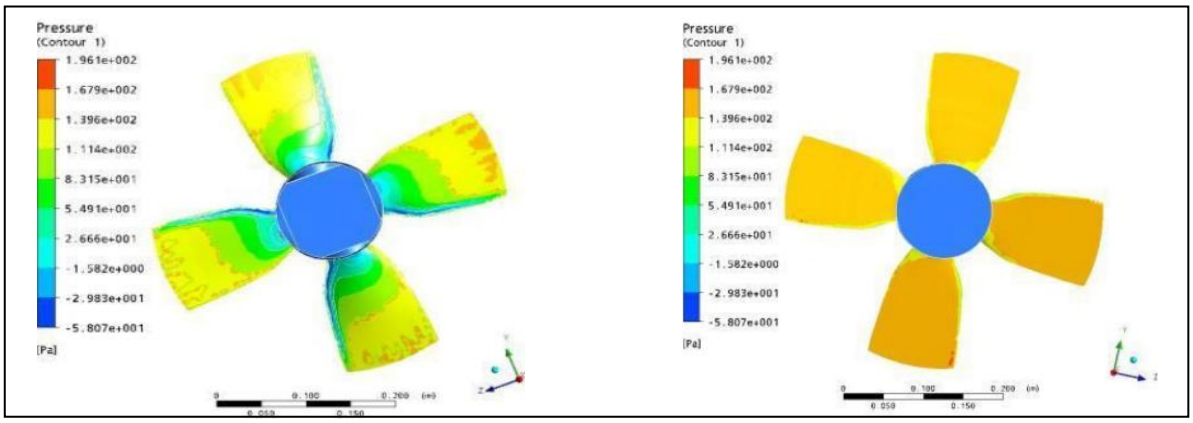

Figure. 7. Pressure Contour at face and back propeller with 4 blades, 225 rpm, d=400 mm, pitch = 0.4

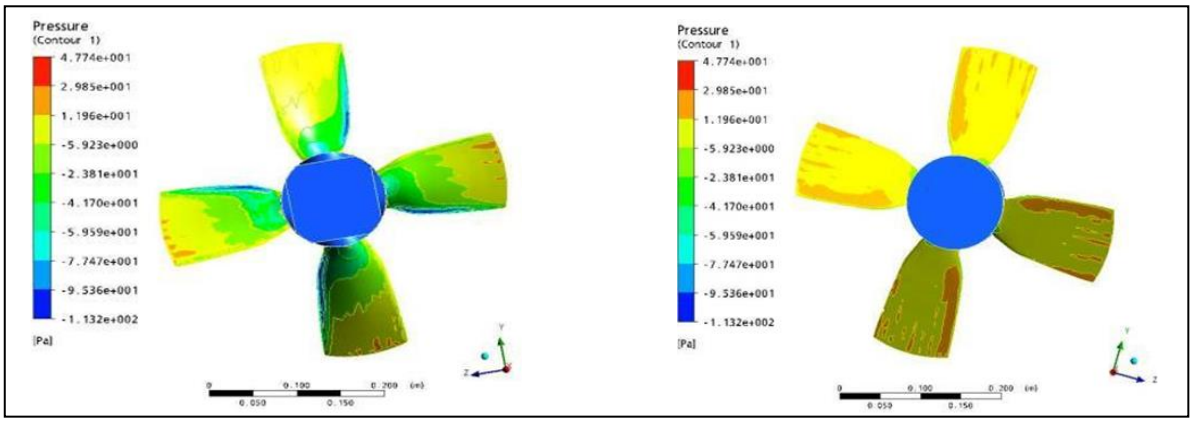

Figure. 8. Pressure Contour at face and back propeller with 4 blades, 225 rpm, d=400 mm, pitch = 0.6

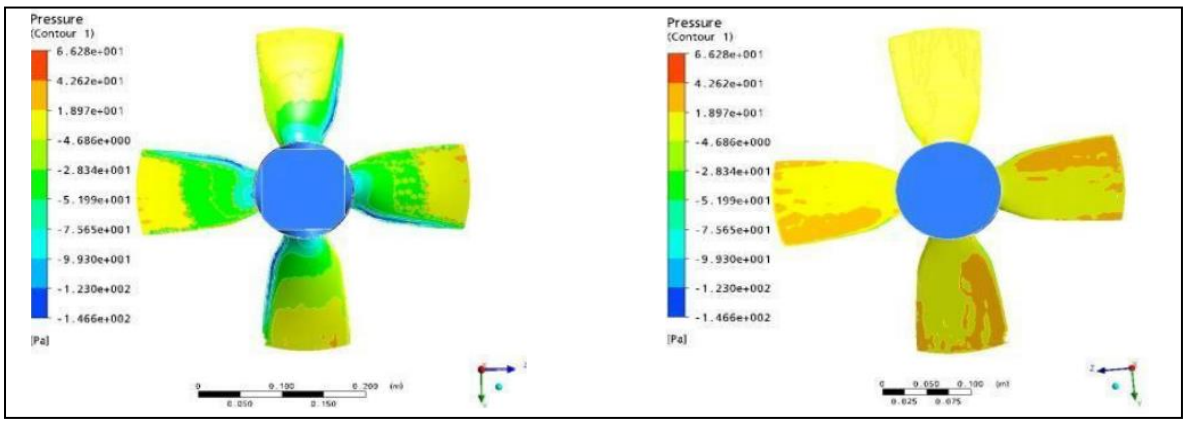

Figure. 9. Pressure Contour at face and back propeller with 4 blades, 225 rpm, d=400 mm, pitch = 0.8

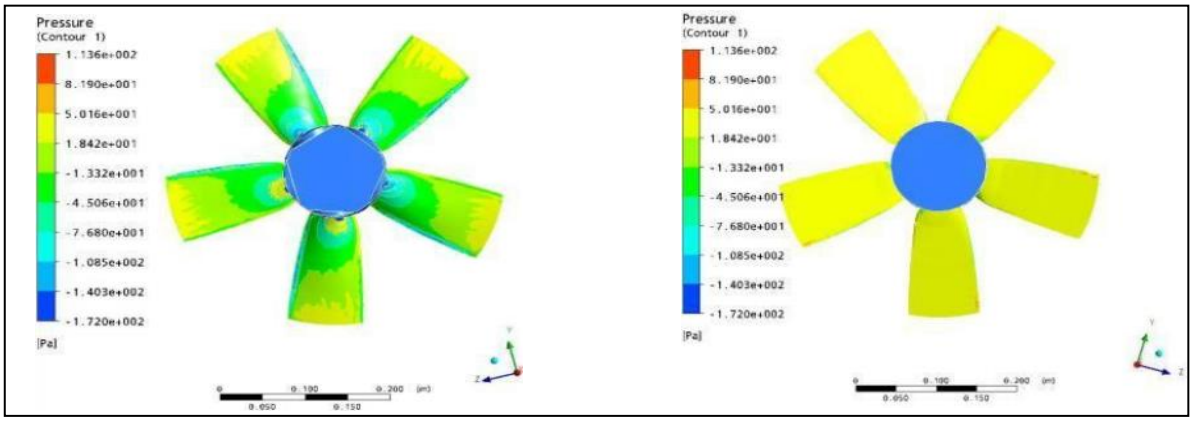

Figure. 10. Pressure Contour at face and back propeller with 5 blades, 225 rpm, d=400 mm, pitch = 0.4

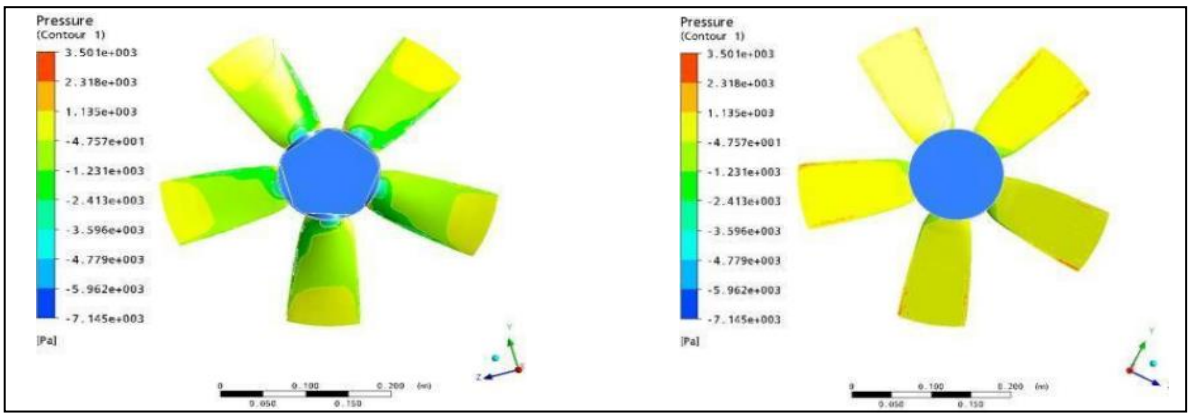

Figure. 11. Pressure Contour at face and back propeller with 5 blades, 225 rpm, d=400 mm, pitch = 0.6

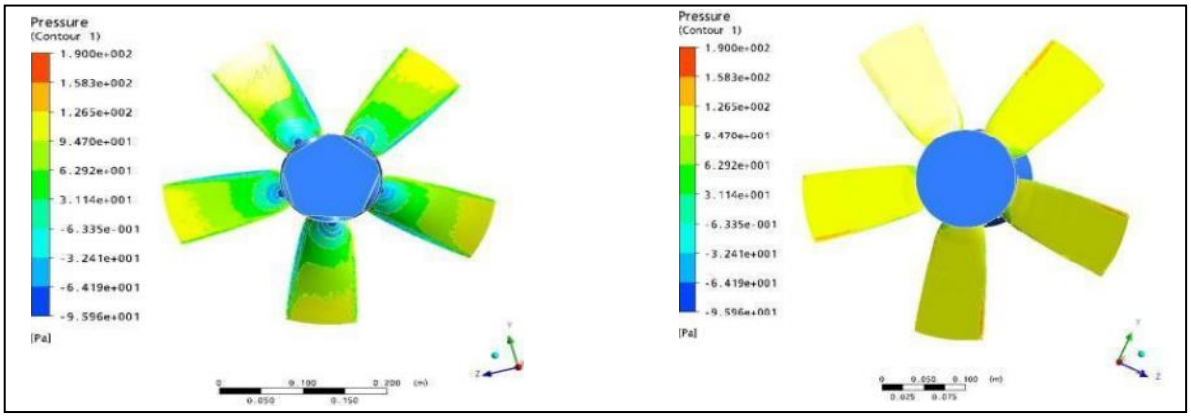

Figure. 12. Pressure Contour at face and back propeller with 5 blades, 225 rpm, d=400 mm, pitch = 0.8

TABLE 2.
PRESSURE RATIO RESULTS FOR D=30 CM WITH VARIATIONS

D (cm)	RPM	Pitch	P-Face (N/m^2)	P-Back (N/m^2)	ΔP (N/m^2)
30	125	0.4	312839	300855	11984
	175	0.4	528349	512349	16000
	225	0.4	959863	937404	22459
	125	0.6	348508	334572	13936
	175	0.6	639036	614639	24397
	225	0.6	998361	961033	37328
	125	0.8	316844	297462	19382
	175	0.8	581393	550106	31287
	225	0.8	904723	852328	52395

TABLE 3.
PRESSURE RATIO RESULTS FOR D=40 CM WITH VARIATIONS

D (cm)	RPM	Pitch	P-Face (N/m^2)	P-Back (N/m^2)	ΔP (N/m^2)
40	125	0.4	451304	437442	13862
	175	0.4	825328	798718	26610
	225	0.4	1292150	1249720	42430
	125	0.6	262679	242086	20593
	175	0.6	474592	436926	37666
	225	0.6	739295	680009	59286
	125	0.8	282493	269772	12721
	175	0.8	509859	485418	24441
	225	0.8	794075	754577	39498

TABLE 4.
PRESSURE RATIO RESULTS FOR D=50 CM WITH VARIATIONS

D (cm)	RPM	Pitch	P-Face (N/m^2)	P-Back (N/m^2)	ΔP (N/m^2)
50	125	0.4	4225940	4163600	62340
	175	0.4	7714560	7604820	109740
	225	0.4	12071600	11900000	171600
	125	0.6	3670830	3655530	15300
	175	0.6	6722070	6699980	22090
	225	0.6	10535000	10504200	30800
	125	0.8	2749170	2736630	12540
	175	0.8	5042490	5012090	30400
	225	0.8	7542030	7480200	61830

2) Discussion

Based on the conducted simulation, it is identified that the pressure ratio on the propeller tends to increase at higher rotation as shown in Tables 2 to 4. For example, at rotation 125 rpm, the ratio of the pressure value between the face and back side is 11984 Pa. At rotation 175 rpm the ratio of the pressure value the face and the back side is 16000 Pa. While at rotation 225 rpm, the value is 22459 Pa. Moreover, the pressure ratio on the propeller tends to increase on the higher pitch at the constant rotation. Whereas at rotation 125 rpm and pitch 0.4 the ratio between the face and back side is 11984 Pa. At pitch 0.6 the value is 13936 Pa. While at pitch 0.8 the value is 19382 Pa, so it is concluded the trend is increasing.

3.2 Propeller Cavitation

1) Propeller Cavitation Analysis

Based on the CFD simulation conducted, can be easily known that the characteristic propensity of each propeller design of each rotation variation. The cavitation that occurred in each propeller can be identified by using the available menu in ANSYS using isosurface CFD. So that the cavitation area can be easily seen and calculated based on the simulation results. The simulation results for design propeller variation (rotation, number of blades, and pitch) on occurred cavitation is represented by the following Figure below.

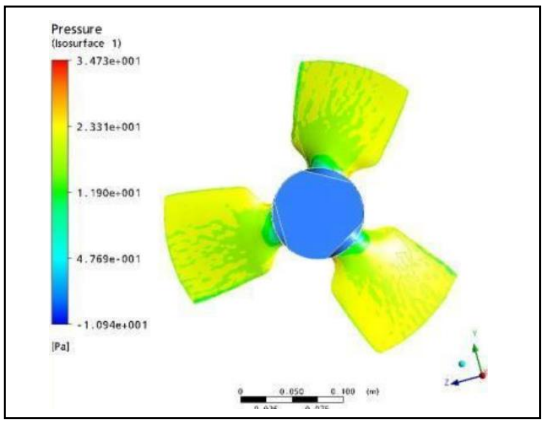

Figure. 13. Propeller cavitation of 3 blades, rotation 125 rpm, d=300 mm, pitch 0.4

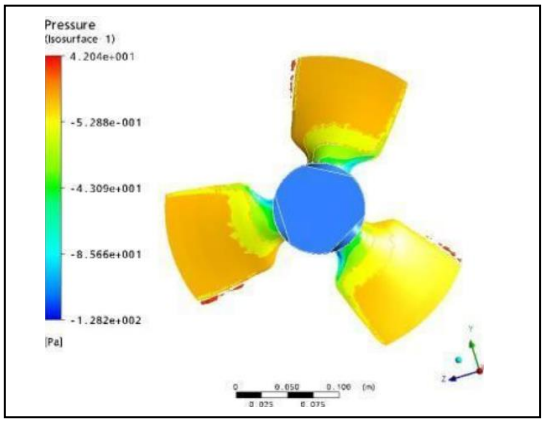

Figure. 14. Propeller cavitation of 3 blades, rotation 175 rpm, d=300 mm, pitch 0.4

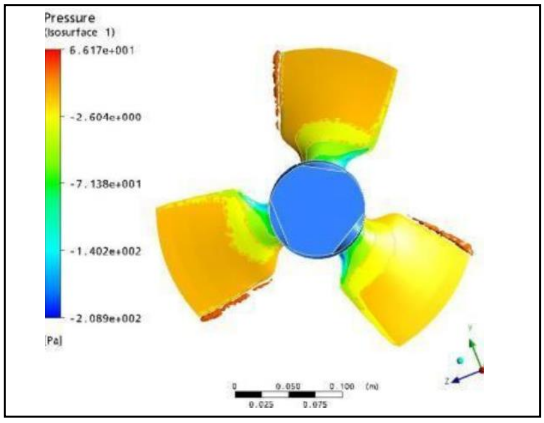

Figure. 15. Propeller cavitation of 3 blades, rotation 225 rpm, d=300 mm, pitch 0.4

Figure 13 to 15 shows the propeller cavitation area from propeller with 3 blades, rotation i.e. 125, 175, and 225 rpm, d = 300 mm, and of pitch 0.4. However, Figure 16 to 18 shows propeller cavitation area from propeller with 4 blades, rotation i.e. 125, 175, and 225 rpm, d = 300 mm, and of pitch 0.4. Furthermore, Figure 19 to 21 shows the propeller cavitation area from propeller with 5 blades, rotation i.e. 125, 175, and 225 rpm, d = 300 mm, and of pitch 0.4. The calculation results of the percentage cavitation area predicted by the simulation of varying propeller geometry are shown by the following Tables 5 to 7 in the next section.

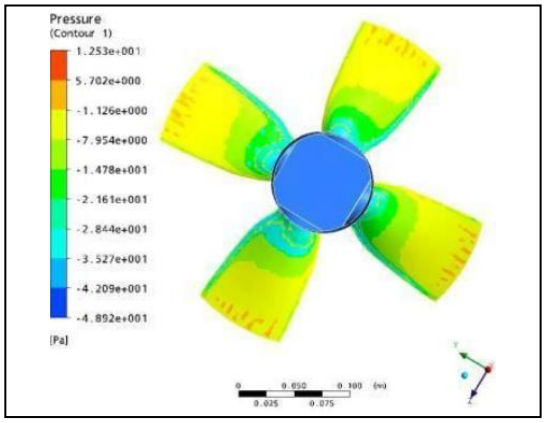

Figure. 16. Propeller cavitation of 4 blades, rotation 125 rpm, d=300 mm, pitch 0.4

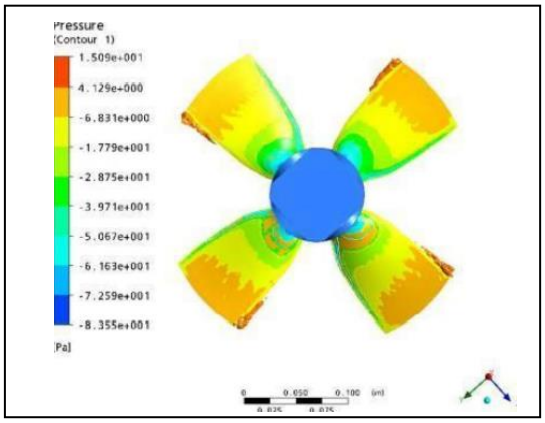

Figure. 17. Propeller cavitation of 4 blades, rotation 175 rpm, d= 300 mm, pitch 0.4

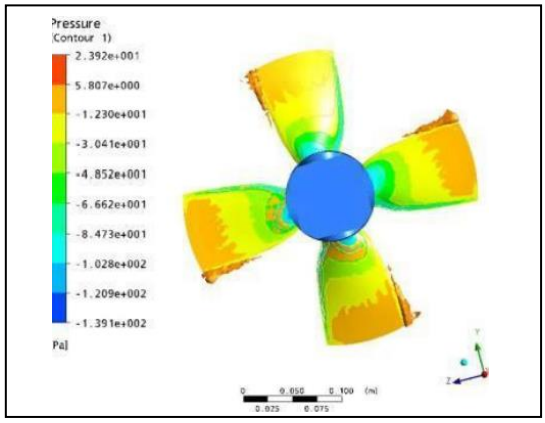

Figure. 18. Propeller cavitation of 4 blades, rotation 225 rpm, d=300 mm, pitch 0.4

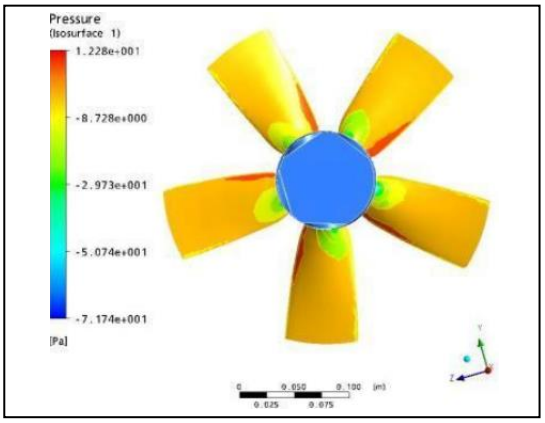

Figure. 19. Propeller cavitation of 5 blades, rotation 125 rpm, d=300 mm, pitch 0.4

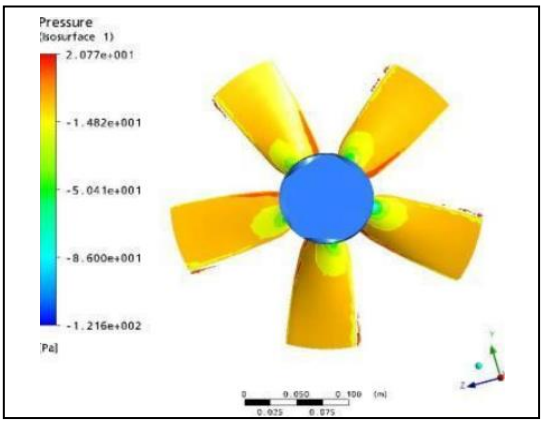

Figure. 20. Propeller cavitation of 5 blades, rotation 175 rpm, d= 300 mm, pitch 0.4

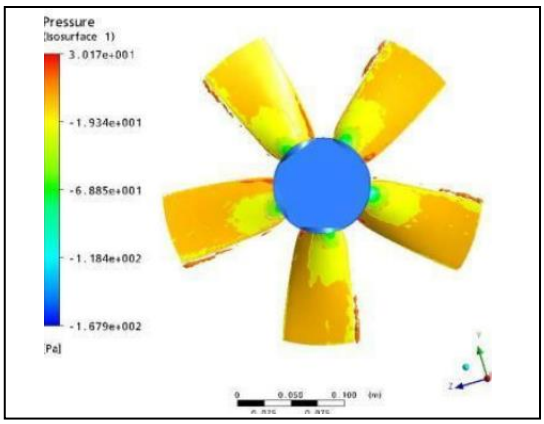

Figure. 21. Propeller cavitation of 5 blades, rotation 225 rpm, d=300 mm, pitch 0.4

TABLE 5.
PERCENTAGE OF CAVITATION AREA FOR 3 BLADES

D (cm)	RPM	Pitch	Total Area (m^2)	Cav. Area (m^2)	%
30	125	0.4	0.0329831	-	-
	175	0.4	0.0329831	0.000476	1.44
	225	0.4	0.0329831	0.001114	3.38
	125	0.6	0.0329831	-	-
	175	0.6	0.0329831	0.000632	1.92
	225	0.6	0.0329831	0.001271	3.85
	125	0.8	0.0329831	-	-
	175	0.8	0.0329831	0.0004644	1.41
	225	0.8	0.0329831	0.0013917	4.22

TABLE 6.
PERCENTAGE OF CAVITATION AREA FOR 4 BLADES

D (cm)	RPM	Pitch	Total Area (m^2)	Cav. Area (m^2)	%
30	125	0.4	0.0329831	-	-
	175	0.4	0.0329831	0.000553	1.68
	225	0.4	0.0329831	0.001655	5.02
	125	0.6	0.0329831	-	-
	175	0.6	0.0329831	0.000370	1.12
	225	0.6	0.0329831	0.002603	7.89
	125	0.8	0.0329831	-	-
	175	0.8	0.0329831	0.0008396	2.55
	225	0.8	0.0329831	0.0029460	8.93

TABLE 7.
PERCENTAGE OF CAVITATION AREA FOR 5 BLADES

D (cm)	RPM	Pitch	Total Area (m^2)	Cav. Area (m^2)	%
30	125	0.4	0.0329831	-	-
	175	0.4	0.0329831	0.000521	1.58
	225	0.4	0.0329831	0.001054	3.20
	125	0.6	0.0329831	-	-
	175	0.6	0.0329831	0.000809	2.45
	225	0.6	0.0329831	0.001990	6.03
	125	0.8	0.0329831	-	-
	175	0.8	0.0329831	0.0018170	5.51
	225	0.8	0.0329831	0.0020600	6.25

2) Discussion

Based on the simulation results as shown in Figure 13 to 21, it can be seen that the cavitation area that occurred on the propeller blade tends to increase on higher rotation. It proved by the calculation results shown in Tables 5 to 7. For example, on the propeller with 3 blades, diameter 300 mm, pitch 0.4 at rotation 125 rpm no indication of cavitation that is 0, then it increases to 1.44% at rotation 175 rpm, and getting higher at rotation 225 rpm to be 4.22% from the total propeller expanding area. Furthermore, on the propeller with 4 blades, diameter 300 mm, pitch 0.4 at rotation 125 rpm no indication of cavitation that is 0, then it increases to 1.68% at rotation 175 rpm, and getting higher at rotation 225 rpm to be 5.02% from the total propeller expanding area. Moreover, on the propeller with 5 blades, diameter 300 mm, pitch 0.4 at rotation 125 rpm no indication of cavitation that is 0, then it increases to 1.58% at rotation 175 rpm and getting higher at rotation 225 rpm into 3.20% from the total propeller expanding area. Besides that, the cavitation area percentage that occurred in the propeller blade tends to increase while the pitch is increased at constant rotation. Whereas at rotation 225 rpm and pitch 0.4 is 3.38 %, then it becomes 3.85 % at pitch 0.6, which is getting bigger at pitch 0.8 that is 4.22 %.

IV. CONCLUSION

From the results of the research of the effect of changes in pitch ratio and the number of blades on cavitation on controllable pitch propeller (CPP), it can be concluded as follows:

1. The pressure ratio on the propeller tends to increase at higher rotation. At rotation 125 rpm, the ratio of the pressure is 11984 Pa, then increase at 175 rpm into 16000 Pa, and getting higher at 225 rpm became 22459 Pa. Moreover, the pressure ratio on the propeller tends to increase on the higher pitch at the constant rotation. At rotation 125 rpm and pitch 0.4, the pressure ratio is 11984 Pa. However, at pitch 0.6 increased to 13936 Pa, and getting higher into 19382 Pa.
2. The cavitation area that occurred on the propeller is influenced by the following variables i.e. the rotation (rpm), diameter propeller (cm), and propeller pitch ratio. The percentage area tends to increase on the higher rotation and also when the pitch ratio is increased at the constant rotation. At rotation 125 rpm the cavitation is 0, then increases into 1.44% at rotation 175 rpm, and getting bigger at 225 rpm into 4.22%. Whereas at rotation 225 rpm and pitch 0.4 the percentage of cavitation area is 3.38 %, then changed into 3.85 % at pitch 0.6, and getting higher at pitch 0.8 into 4.22 %.

REFERENCES

[1] Chaosheng Zheng, Dengcheng Liu, and Hongbo Huang. "*The Numerical Prediction and Analysis of Propeller Cavitation Benchmark Tests of YUPENG Ship Model*" Journal of Marine Science and Engineering. J. Mar. Sci. Eng. 2019, 7, 387; doi:10.3390/jmse7110387. 2019.

[2] Shinagam Rama Krishna et al., 2012. "CFD Analysis of a Propeller Flow and Cavitation". International Journal of Computer Applications (0975 – 8887). Volume 55– No.16, October 2012.

[3] Salvatore, F., Testa, C., Ianniello, S. and Pereira, F.2006. Theoretical modeling of unsteady cavitation and induced noise, INSEAN, Italian Ship Model Basin, Rome, Italy, Sixth International Symposium on Cavitation, CAV2006, Wageningen, The Netherlands.

[4] Fujiyama, K.; Nakashima, Y. Numerical Prediction of Acoustic Noise Level Induced by Cavitation on Ship Propeller at Behind-Hull Condition. In Proceedings of the 5th Symposium on Marine Propulsors, SMP'17, Espoo, Finland, 12–15 June 2017; pp. 739–744.

[5] Kawakita, C. et al. "CFD on Cavitation around Marine Propellers with Energy-Saving Devices", Mitsubishi Heavy Industries Technical Review Vol. 49 No. 1 (March 2012)

[6] Long, Y.; Long, X.; Ji, B.; Huang, H. Numerical simulations of cavitating turbulent flow around a marine propeller behind the hull with analyses of the vorticity distribution and particle tracks. Ocean Eng. 2019, 189, 106310.

[7] Pereira, F., Salvatore, F., and Di Felice, F. (2004). Measurement and modeling of propeller cavitation in uniform inflow, J. of Fluids Engineering, Vol. 126, pp 671-679.

[8] Pereira J. C. F. and Sequeira, A. 2010. Propeller-flow predictions using turbulent vorticity-confinement, V European Conference on Computational Fluid Dynamics, ECCOMAS CFD 2010, Lisbon, Portugal.

[9] Arifin, M.D. et al. "*Analisa Pengaruh Perubahan Pitch Ratio dan Jumlah Blade Terhadap Kavitasi Pada Controllable Pitch Propeller (CPP)*" Jurnal Teknik Vol IX No 2 September 2019.

[10] Arifin, M.D. et al. "*Analisa Kavitasi Terhadap Perubahan Kerja Pitch dan Jumlah Blade Pada CPP*" Surabaya, 2010.

[11] Adji, S.W. *"Vessel Resistance".* Text Modules of vessel propulsion subject. Jurusan Teknik Sistem Perkapalan, Fakultas Teknologi Kelautan, ITS. Surabaya. 2001

[12] Adji, Suryo W. "*Propeller Design*". Text Modules of Propulsion Subject. Jurusan Teknik Sistem Perkapalan, Fakultas Teknologi Kelautan, ITS. Surabaya. 2001

[13] Carlton, John. "*Marine Propeller and Propulsion*". Oxford University: Elsevier, 2007.

[14] Harvald, Sv. Aa." *Propulsion and Resistance of Vessel". Surabaya: Airlangga University Press.* 1992. DOI:10.1016/0191-2607(84)90024-4

[15] Tutug Triasniwan. 2010. "*Software Design Study for identification Analysis of Propeller Cavitation*". http://digilib.its.ac.id/public/ITS-Undergraduate-12495-Paper.pdf